Open Access

Assessment of a Numerical Approach Suitable for the M2P2 Problem

M. Pfeiffer*[,1], D. Petkow[2], G. Herdrich*[,1] and S. Fasoulas*[,1]

[1]Institute of Space Systems, University of Stuttgart, Pfaffenwaldring 31, D-70569 Stuttgart, Germany

[2]Advanced Concepts Team, ESA-ESTEC, Keplerlaan 1, 2200 AG Noordwijk, The Netherlands

Abstract: The magnetic sail is a quite new concept of space propulsion utilising the solar wind in order to transfer momentum to a magnetic field source. The magnetic field size can be increased significantly by injecting a plasma into the center of the magnetic bubble. This concept is called Mini-Magnetospheric Plasma Propulsion (M2P2) system. The plasma injection shall create a magnetosphere with a diameter of several km. Because of these large scales, experiments are difficult and most of the published studies on this concept are therefore based on numerical investigations. The applied approaches, MHD and hybrid (MHD/kinetic), are analysed in the context of the strongly diverging results in the published studies on e.g. magnetic field decay. A validity parameter (Damköhler number) for the simulation methodologies is proposed and also an analytical estimation of basic M2P2 characteristics is presented. Finally, a recommendation is given for future M2P2 simulation methodologies which, for the sake of accuracy, should base on purely kinetic approaches.

Keywords: M2P2, magnetic sail, hybrid simulation, fully kinetic simulation.

1. INTRODUCTION

For future space missions, e.g. to the outer solar system or to Mars [1, 2], a propulsion system is needed with an optimal speed to mass/energy ratio. The Mini-Magnetospheric Plasma Propulsion (M2P2) system promises to be such a propulsion system, having a very low propellant demand since it makes use of the natural solar wind to create thrust. However, a large scale magnetosphere with the size of several km is needed in order to intensify the interaction with the charged particles emitted by the Sun. The enlargement of the magnetic bubble might be achieved by injecting a plasma into the magnetic field of a central coil (see Fig. **1**).

Several authors have already reported on this new technology [3-5]. However, there are only a few experiments of the M2P2 system due to the large scales and the associated problems in laboratories. The experiments by Winglee *et al*. [6] and Funaki *et al*. [5, 7, 8] give a qualitative picture of the magnetosphere but they cannot make a description of characteristics, parameters, or the evolution of the magnetosphere after the plasma injection. So far, the only way for a study is to use a high fidelity numerical approach.

In previously performed M2P2 simulations [4, 9, 10] some unresolved issues are left due to inconsistencies and differences in the reported results. As an example, the simulation results obtained by Winglee *et al*. [9] and by Khazanov *et al*. [4] differ with respect to the extended magnetic field size: the final magnetosphere by Winglee *et al*. has a diameter of about 20 km in contrast to the final magnetosphere by Khazanov *et al*. with a diameter of about 80 km, although the same initial and boundary conditions have been used by both. Most authors use either a magnetohydrodynamic (MHD) approach, or a hybrid methodology (MHD and kinetic approach). As it will be shown later, the pure MHD approach cannot be applied for the simulation of the M2P2 system due to wide range of spatial scales.

This article concentrates on the discussion of the M2P2 system, focusing on the state of the art of the applied numerical methods. The validity of the different approaches is clarified with respect to spatial scale concerns. As a pre-requisite, the original idea of the magnetic sail concept proposed by Zubrin [11] is also briefly described and studied analytically. A brief introduction to the fundamentals and working principles of the M2P2 concept with focus on momentum transfer, i.e. on force estimation, is followed by a description of the different simulation approaches including a discussion on a validity condition for MHD and a hybrid approach. Finally, basic requirements for an M2P2 simulation approach are derived.

2. MAGNETIC SAIL CONCEPT

The propulsion concept of the magnetic sail makes use of the momentum transfer to a spacecraft caused by deflecting charged solar wind particles by a strong magnetic field. The original idea was proposed by Zubrin [11]. Therein, a coil is used to generate a magnetic field and to deflect the solar wind particles. The main problem of this concept is the necessity for very large coil diameters and currents in order to produce a large interaction cross section between the magnetic field and the solar wind particles. However, a large interaction cross section is essential for the generation of a non-negligible momentum transfer to the spacecraft. The numerical values used by Zubrin have been

*Address correspondence to these authors at the Institute of Space Systems, University of Stuttgart, Pfaffenwaldring 31, D-70569 Stuttgart, Germany; Tel: 0711 68562375; Fax: 0711 68563596;
E-mails: mpfeiffer@irs.uni-stuttgart.de,
herdrich@irs.uni-stuttgart.de, dejan.petkow@esa.int,
fasoulas@irs.uni-stuttgart.de

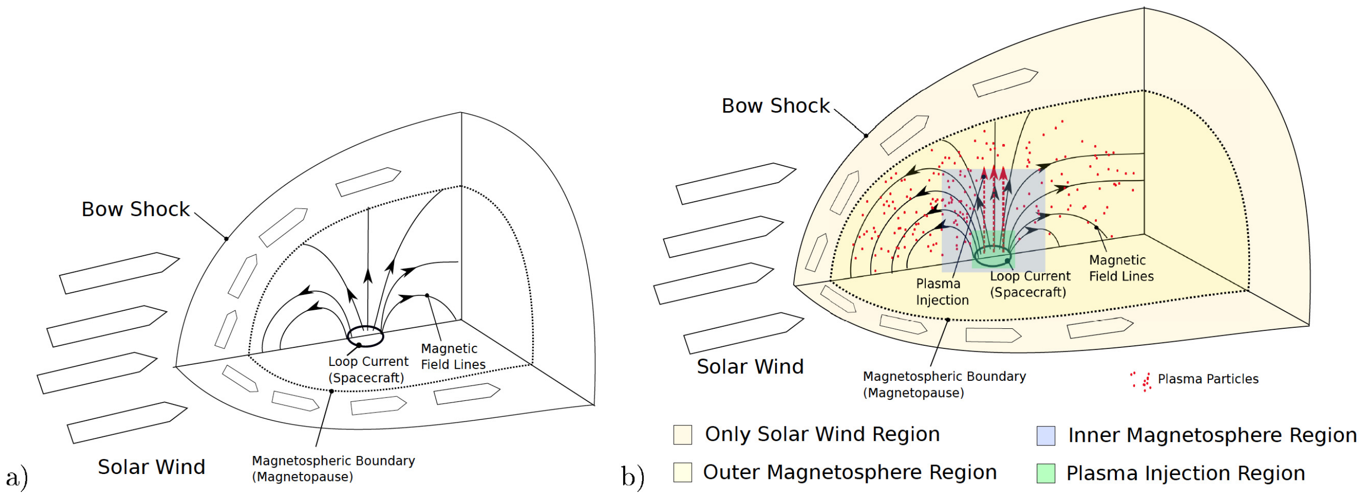

Fig. (1). Schematics of the magnetic sail: **a**) without plasma injection and **b**) with plasma injection and enlarged magnetosphere. The differences in size are only qualitative character.

- coil diameter $d_{coil} = 31.6$ km,
- number of coil turns $n_{coil} = 1$,
- coil current $I_{coil} = 50$ kA,

and the demand for a superconducting coil.

The mass is indeed one of the key problems of the concept. Zubrin estimates the mass of the coil to about $m_{coil} \approx 5$ t. However, the biggest challenge is probably the dimension of the coil - a wire formed as a coil with a diameter of approximately 32 km (!) has to be placed in space in a stable position. This is structurally and mechanically indeed a challenge.

2.1. Simple Force Estimation

Zubrin has made simple estimations of the force on the spacecraft. Here, additional considerations needed for discussing the M2P2 system in detail are presented.

After turning on the coil current, a magnetic field around the spacecraft is built. Charged particles of the solar wind are deflected by this magnetic field. The resulting pressure of the solar wind particles deforms the magnetic field lines. Subsequently, the magnetic field is pushed back until the magnetic pressure p_{mag} equals the dynamic pressure p_{SW} of the solar wind.[1] Thus, it follows:

$$p_{SW} = p_{mag} \Rightarrow \rho_{SW} v_{SW}^2 = \frac{B^2}{2\mu_0}. \tag{1}$$

Here, ρ_{SW} is the solar wind density, v_{SW} is the velocity of the solar wind particles, B the magnetic field of the coil and $\mu_0 = 4\pi \cdot 10^{-7}$ H/m the magnetic constant.

Solar wind consists mainly of hydrogen nuclei (protons) and electrons. Most of the other particles are α-particles ${}_2^4\mathrm{He}^{2+}$. They represent about $2-5\%$ of the total particle number [12, 13]. For simplicity, it is therefore assumed that the solar wind consists only of protons and electrons. Considering then the solar wind in a distance of 1 AU, the mean values for the fast and slow particles are given in Table **1** (the small differences in the volume density of electrons and protons at 1 AU can be neglected, the mass density is crucial [12, 13]).

Table 1. Selected Properties of the Solar Wind at 1 AU

	Slow SW	Fast SW
v_{SW} [m/s]	$3.5 \cdot 10^5$	$6,7 \cdot 10^5$
ρ_{SW_p} proton [kg/m³]	$1.8 \cdot 10^{-20}$	$5.0 \cdot 10^{-21}$
ρ_{SW_e} electron [kg/m³]	$9.8 \cdot 10^{-24}$	$2.7 \cdot 10^{-24}$
p_{SW_p} [Pa]	$2.2 \cdot 10^{-9}$	$2.3 \cdot 10^{-9}$
p_{SW_e} [Pa]	$1.2 \cdot 10^{-12}$	$1.2 \cdot 10^{-12}$

This leads to the following conclusions:

1. The dynamic pressures of both slow and fast solar wind particles are almost identical at 1 AU. Thus, in the following estimations a consideration of the composition of the solar wind is not necessary.
2. The pressure caused by the protons is crucial for the expression of the magnetopause, i.e. for the position at which the magnetic pressure equals the dynamic pressure of the solar wind, $p_{SW} = p_{mag}$. The pressure of the electrons can be neglected.

It is now essential to have an information about the magnetic field $\vec{B} = \vec{B}(\vec{r})$ at a position $\vec{r}$ to estimate the

[1]The magnetic pressure of the solar wind is neglected: $p_{mag,SW} \approx p_{SW} \cdot 10^{-3} \Rightarrow p_{mag,SW} \ll p_{SW}$ [12].

magnetic pressure. If it is assumed that the coil is a dipole[2] it follows

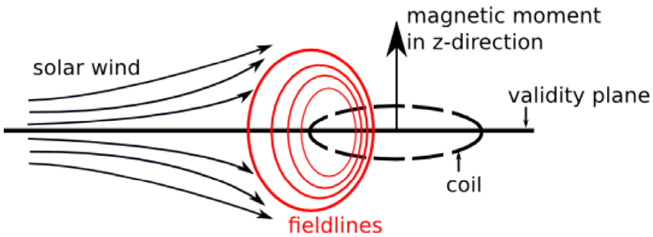

Fig. (2). Interaction of the solar wind with the magnetic field.

$$\vec{B}(\vec{r}) = \frac{\mu_0}{4\pi} \frac{3\vec{r}(\vec{m}\cdot\vec{r}) - \vec{m}r^2}{r^5}. \tag{2}$$

Here, $\vec{r}$ is the distance from the magnetic dipole moment $\vec{m}$. If the equatorial plane of the coil surface is considered in the estimation only (see Fig. **2**), then $\vec{m} \perp \vec{r} \Rightarrow \vec{m}\cdot\vec{r} = 0$ and so

$$\vec{B}(\vec{r}) = -\frac{\mu_0 \vec{m}}{4\pi r^3}. \tag{3}$$

Inserting this result in equation (1) yields for the distance of the magnetopause R_{MP} (see Fig. **1**)

$$R_{MP} = \left(\frac{\mu_0 m^2}{32\pi^2 p_{SW}}\right)^{1/6}. \tag{4}$$

Assuming that the interaction area of the magnetic field and the solar wind is about the circle with the area πR_{MP}^2, the resulting force F_{MP} on the magnetic field (acting at the magnetopause) and also on the spacecraft is then about

$$F_{MP} \approx p_{SW}\pi R_{MP}^2 = \left(\frac{\pi\mu_0}{32} m^2 p_{SW}^2\right)^{1/3}. \tag{5}$$

The magnetic moment of a current carrying coil is the product of the number of turns n, the current I and the surface of the coil $\vec{A}$: $\vec{m} = n\cdot I\cdot\vec{A}$. The resulting force which would act on the spacecraft is then $F_{MP} \approx 280\ \text{N}$ using the values given by Zubrin, see [11]. However, the values proposed by Zubrin are very optimistic. Therefore, this result should be considered only as a theoretical value with a correspondingly high uncertainty. The estimation contains additional simplifications that were not discussed so far:

- The magnetic field of the coil is more a multipole field than a dipole field. Thus, the real initial magnetic field $\vec{B}(\vec{r})$ has a different shape.
- In the calculation of F_{MP} it is assumed that all particles are deflected by the circle with radius R_{MP}. This is certainly not the case. A factor $\varepsilon \in [0,1] = \varepsilon_1 \cdot \varepsilon_2$ should be introduced where
  - ε_1 gives the relative percentage of the momentum transferring particles and
  - ε_2 represents the relative percentage of the momentum transferred to the magnetosphere.

  In a sense these two parameters describe the coupling efficiency between the magnetic bubble and the solar wind. Eventually, the introduction of a third parameter ε_3 might be useful which gives the percentage of the momentum transferred to the spacecraft compared to the momentum transferred to the magnetosphere. This parameter should equal unity in case of a steady-state condition as it contains information on the currently occurring deformation of the magnetosphere.
- The circle with radius R_{MP}, i.e. the interaction cross section between the solar wind and the magnetic field, is outside the equatorial plane of the coil.

However, the largest problem originates from the ansatz for the force itself: The formulation is based on the pure fluid assumption. Its validity is questionable since currents and electromagnetic forces cannot be neglected, they are the fundamental quantities which strongly interfere with the fluid.

2.2. Lorentz Force Acting on the Spacecraft

The Lorentz force with the force density

$$\vec{f} = \vec{j}_{coil} \times \vec{B}_{ext} \tag{6}$$

is the only force which acts directly on the spacecraft. Here, $\vec{j}_{coil}$ is the coil current density and $\vec{B}_{ext}$ is the magnetic field caused by the interaction between the solar wind and the magnetic bubble. This interaction induces currents which itself create additional magnetic fields $\vec{B}_{ext}$. The used current system is the Chapman-Ferraro type [14]. This system is located in the magnetopause and separates the solar wind from the magnetic field of the coil.

For an analytical estimation of the force F_{SC} acting on the spacecraft, some approximations are introduced according to Toivanen *et al.* [15]. First, again it is assumed that the magnetic field of the coil is a dipole field in z-direction. Therefore, $\vec{m} = m\vec{e}_z$ and $\vec{m}$ is point-shaped, and the current density of the coil is

$$\vec{j} = \nabla \times (\vec{m}\,\delta(\vec{r})). \tag{7}$$

Here, ∇ is the Nabla operator and $\delta(\vec{r})$ is the 3-d Dirac delta function. The resulting total force on the spacecraft is

$$F_{SC} = \int \vec{j} \times \vec{B}\, d^3\vec{r} = \int (\nabla \times \vec{m}\,\delta(\vec{r})) \times \vec{B}\, d^3\vec{r}. \tag{8}$$

Considering only the force in x-direction (let this be also the solar wind direction), it follows

$$F_{SC_x} = m\frac{\partial B_z(0)}{\partial x}, \tag{9}$$

Thus, the force is a product of the dipole moment and the gradient of the induced magnetic fields at the location of the dipole moment. The gradient $\partial_x B_z$ cannot be solved

[2]Looking at a magnetic field from a large distance makes the multipole parts small compared with the dipole part.

analytically as the location and amplitude of the produced currents are not clear. Even in case these values are known, the calculation would not be trivial.

However, it is possible to give a rough dependence of the force, assuming that the Chapman-Ferraro is still the dominant current system. This current has a distance from the dipole (i.e. the spacecraft) of R_{MP}. Thus, the gradient of the magnetic field produced by this current is $\partial_x B_z(0) \sim B_{MP} / R_{MP}$ at the location of the dipole. Equation (1) with $B = B_{MP}$ and equation (4) give then the proportionality relation of the force, i.e.

$$F_{SC_x} \sim \frac{B_{MP}}{R_{MP}} \sim \left(\mu_0 m^2 p_{SW}^2\right)^{1/3}. \tag{10}$$

This dependence is identical for both approaches if the pre-factors are neglected.

3. CURRENT STATE OF M2P2 RESEARCH

The simple magnetic sail concept based on a coil is currently not feasible due to the problems indicated above. Winglee *et al*. [3, 9] proposed therefore to inject a plasma from a plasma source into the magnetic field in axial direction (see Fig. **1**: plasma injection region). In the vicinity of the plasma injection the MHD equations are certainly valid (detailed explanations will follow later, see subsection 3.1). Thus, the MHD approach can be used for a first evaluation of the M2P2 concept. From Faraday's and Ohm's laws, it follows

$$\nabla \times \frac{\vec{j}}{\sigma} - \nabla \times \left(\vec{v} \times \vec{B}\right) = -\frac{\partial \vec{B}}{\partial t} \tag{11}$$

with the plasma velocity $\vec{v}$, the current density $\vec{j}_{coil}$, the electric conductivity σ and the magnetic field $\vec{B}_{coil}$. Using equation (11) with Ampéres simplified law

$$\nabla \times \vec{B} = \mu_0 \vec{j} \tag{12}$$

(the displacement current is neglected) leads to the induction equation

$$\begin{aligned} \frac{\partial \vec{B}}{\partial t} - \nabla \times \left(\vec{v} \times \vec{B}\right) &= -\frac{1}{\sigma\mu_0} \nabla \times \left(\nabla \times \vec{B}\right) \\ &= -\frac{1}{\sigma\mu_0}\left(grad\left(\nabla \cdot \vec{B}\right) - \Delta \vec{B}\right) \\ &= \frac{1}{\sigma\mu_0} \Delta \vec{B} \end{aligned} \tag{13}$$

as $\nabla \cdot \vec{B} = 0$. Equation (13) and also the ratio of the $\left|\nabla \times \left(\vec{v} \times \vec{B}\right)\right| \approx vB / L$ term and the $\left|\Delta \vec{B}\right| \approx B / L^2$ term (L: characteristic system length) are a measure for the deformation of $\vec{B}$. This ratio yields the so-called magnetic Reynolds number Re_m [16-18]:

$$Re_m = \frac{\left|\nabla \times \left(\vec{v} \times \vec{B}\right)\right|}{\frac{1}{\sigma\mu_0}\left|\Delta \vec{B}\right|} \approx \sigma\mu_0 v L. \tag{14}$$

The magnetic Reynolds number represents a dimensional analysis of the term coefficients in equation (14) and, therefore, allows the statement whether the flow and the magnetic field configuration have to be treated in a coupled way or not. For example, the condition $Re_m \gg 1$ characterizes so-called "frozen-in" situations where magnetic lines are carried by the moving fluid, so that the magnetic field is deformed. The result of this deformation is an enlargement of the magnetosphere. Subsequently, the proportionality of the magnetic field changes from $B \sim 1 / r^3$ (r: distance) to $B \sim 1 / r^k \mid k < 3$ without changing the dipole strength. The value of k is still not clarified.

Also the optimal choice of the plasma source for a greatest possible expansion of the magnetic field is not clarified. Currently, we derive only one constraint concerning the plasma source in the centre of M2P2 - the source should be optimized to work with Hydrogen. In order to get close to the propellantless working principle, the plasma source should be an open system as plasma particles would enter the system from the poles where the particle's origin is either the source itself or the surrounding solar wind. In this sense one can probably identify a refuelling mode of operation as initially propellant will be needed for extending the magnetic field line distribution.

3.1. MHD Approach

The fundamental problem in numerical studies is not the geometrical size of the M2P2 system, but the differences in spatial scales relevant for the underlying model approach. These scales range from some cm at the injection up to a size of some km of the magnetosphere. Winglees simulation is based on the MHD approach. The code he used was originally developed for the simulation of the Earth's magnetosphere. However, the MHD method can only deal with scale differences of about 10^3 in the simulation area. M2P2 covers scale differences of $> 10^5$, so a system of nine subgrids was implemented by Winglee. Every subgrid is surrounded by the next greater subgrid. Every sub grid contains the same cell number ($50 \times 40 \times 40$) but each cell of a subgrid is only half as large as the cells of the corresponding supergrid. Each subgrid contains the inner boundary conditions for the corresponding supergrid and each supergrid contains the outer boundary conditions for the corresponding subgrid. The dimension of the largest grid is 10 km, the radius of the smallest is 10 m.

Winglee used then an extrapolation to obtain a relation between the magnetic field of the coil and the size of the magnetosphere. He assumed a small magnetic field $B = 1\ \mu\mathrm{T}$ in the smallest subgrid and injected a plasma with a velocity of $v_{pl} = 20$ km/s from the spacecraft (represented by a ball with radius of 5 grid points). After the simulation has started and equilibrium was reached, the size of the magnetosphere was determined. This process was then repeated for $B = 2\ \mu\text{T}$ and $B = 4\ \mu\text{T}$. In the next step, the relation between size of magnetosphere and magnetic field was extrapolated until the magnetosphere reached a size of 20 km. Given that, the required magnetic field for the extrapolation at a radius of 10m (smallest subgrid) was found to be about $B \approx 0.6 - 0.7$ mT. This magnetic field was scaled down to the required size of 0.1 m (size of the jet nozzle). In order to create a magnetosphere of 20 km, according to Winglee, only a 10 cm coil is needed which generates a magnetic field of $B \approx 60 - 70\ \mu\text{T}$ at the position of the dipole. Then, the relation between magnetic field B and distance r would correspond to $B \sim 1/r$ as a result of the plasma injection. This results can be described better if one applies the following assumption [15]:

$$B_r = B_0 \left(\frac{L}{r}\right)^k, \tag{15}$$

$$B_0 = \frac{\mu_0 m}{4\pi L^3}. \tag{16}$$

Here, L is the coil diameter, r is the distance from the dipole (coil), m is the magnetic dipole moment and k is the order of decrease of magnetic induction B as a function of distance. One could say that B behaves normally up to the edge of the coil, i.e. $B \sim 1/r^3$. Then, there is another relation due to the plasma injection and it can be expected that $k < 3$, e.g. in the case of Winglee $k = 1$.

Unresolved Issues in the MHD Approach. The extrapolation and the scale differences should be discussed critically. It is not sure that such an extrapolation from large to small scales can be performed without loss of physical accuracy, for a detailed discussion see [4].

Also, a problem with respect to the conservation of magnetic flux in connection with the extrapolated decrease parameter $k = 1$ in [9] is described in [19]. The magnetic flux Φ_{in} in the coil with radius L and the magnetic induction B_0 is given by

$$\Phi_{in} = \pi L^2 B_0.$$

For the external magnetic flux one should have

$$\Phi_{out} = \int_0^{2\pi}\int_L^R r B(r)\, d\varphi\, dr = \Phi_{in}$$

due to flux conservation. However, the estimation in case of $k = 1 \Rightarrow B(r) = B_0 \frac{L}{r}$ leads to

$$2\pi B_{MP} R^2 = \pi L^2 B_0 \tag{17}$$

$$\Rightarrow B_{MP} = \frac{B_0}{2}\frac{L^2}{R^2}. \tag{18}$$

This can have three reasons according to [19]:

- Φ is not conserved in the simulation,
- Φ is conserved but there are failures in the scaling,
- the proportionality $B \sim 1/r$ is not only caused by the interaction between dipole and plasma injection. It is rather a consequence of the interaction between dipole, plasma injection *and* solar wind.

Another related problem affects the assumption of the general validity of the MHD equations on all spatial scales. One condition concerns the gyration radius of the ions,

$$r_g = \frac{m_{par} v_\perp}{|q| B}. \tag{19}$$

Here, $v_\perp$ is the velocity component of the particles perpendicular to the magnetic field and m_{par} is the mass of the particles. The gyration radius needs to be smaller than a characteristic length l of the plasma system [20]. Hence, the MHD equations are *per se* not valid everywhere in the simulation domain. Two examples:

- At a distance of 10 m to the plasma injection, there are many particles with velocity components perpendicular to the magnetic field lines. These components arise from the beam divergence of the plasma jet and the characteristics of the magnetic field lines at this distance. At the plasma jet injection the characteristic length equals the size of the subgrid, $l = 10$ m. Winglee assumes that there are particles with velocity $v_\perp = 20$ km/s. This leads to the following magnetic induction strengths which were also used by Winglee for the extrapolation:

  $$B = 1\ \mu\text{T} \Rightarrow r_g \approx 200 \text{ m}$$
  $$B = 2\ \mu\text{T} \Rightarrow r_g \approx 100 \text{ m}$$
  $$B = 4\ \mu\text{T} \Rightarrow r_g \approx 50 \text{ m}.$$

  The condition $r_g < l$ is obviously not met here. For the final value of $B = 600\ \mu\text{T} \Rightarrow r_g \approx 0.43$ m the simulation is valid but this value results from an extrapolation in which the condition is not met. Additionally, not every particle has a velocity of $v_\perp = 20$ km/s, it could be worth clarifying how many particles really have a velocity of that magnitude.
- The solar wind particles have a velocity of $v_{SW} \approx 400$ km/s towards the magnetosphere of $l = 15$ km. The interplanetary magnetic field (IMF) has a magnitude of about $B \approx 1 - 10$ nT [14], so the gyration radius of the solar wind particles is about $r_g \approx 200 \text{ km} > l$. Thus, a MHD approach is not valid in the outer region of the magnetosphere (see Fig. **1**).

3.2. Hybrid Approach

Khazanov *et al.* [4] applied a hybrid approach consisting of a MHD and a kinetic/fluid description. The computational domain was decomposed as follows:

1. The inner region is dominated by the plasma source. The simulation was performed with a MHD code and with a magnetic field of $B = 600\ \mu\mathrm{T} \Rightarrow l > r_g$.

2. The outer region is dominated by the solar wind. This area was computed with a hybrid approach where the electrons were treated as a fluid (smaller mass $\rightarrow$ smaller gyration radius), and the ions as particles.

The hybrid simulation represents indeed a significant improvement compared to a pure MHD simulation as used by Winglee. As a consequence, the results of both simulations are very different, e.g. the sizes of the magnetospheres with the same parameters: $r_{Wing} = 20\ \mathrm{km} < r_{Khaz} = 80\ \mathrm{km}$. There are also qualitative differences, e.g. the dependence of the magnetic field to the distance in the inner region $B \sim 1/r^2$ in the hybrid simulation, whereas Winglee $B \sim 1/r$ in the MHD approach.

Unresolved Issues in the Hybrid Simulation Approach. Having two different approaches in one simulation usually creates other problems:

- Khazanov defined a static border between the domains at a distance of 25 km. However, it is not known *a priori* at which position the domain border should be placed. Also, it is not known *a priori* which shape this boundary should possess.
- The computations were performed subsequently. The first simulation delivered the (inner) inflow and boundary conditions for the outer domain. Therefore, the coupling is of one way type, i.e. there is an information transfer from the inner region to the outer region, but there is no information transfer from the outer region to the inner region, not even for the electrons which are the main carriers of the currents in the magnetosphere.

3.3. Comparative Force Estimates

The results reported by Winglee can be understood better if one applies the results given in Sec. 2.1 in combination with the equations (15) and (16) of Toivanen *et al.* [15].

Then, the following function for $R_{MP_{M2P2}}$ can be derived:

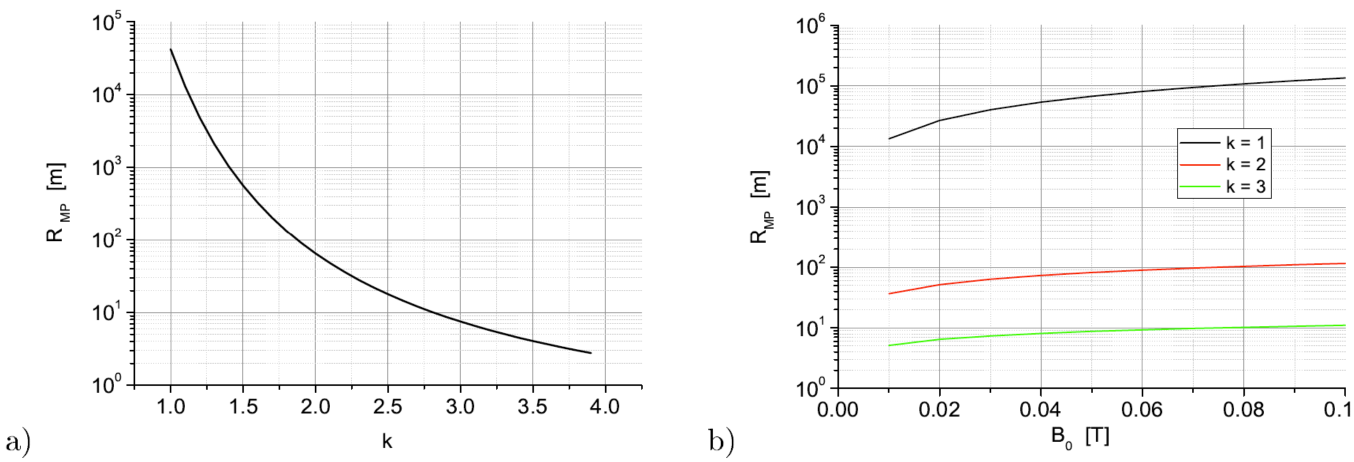

Fig. (3). $R_{MP_{M2P2}}$ based on the values of Winglee and the following relations (see section 3.3): **a)** $R_{MP_{M2P2}}(k)$ and **b)** $R_{MP_{M2P2}}(B_0)$ for different *k*.

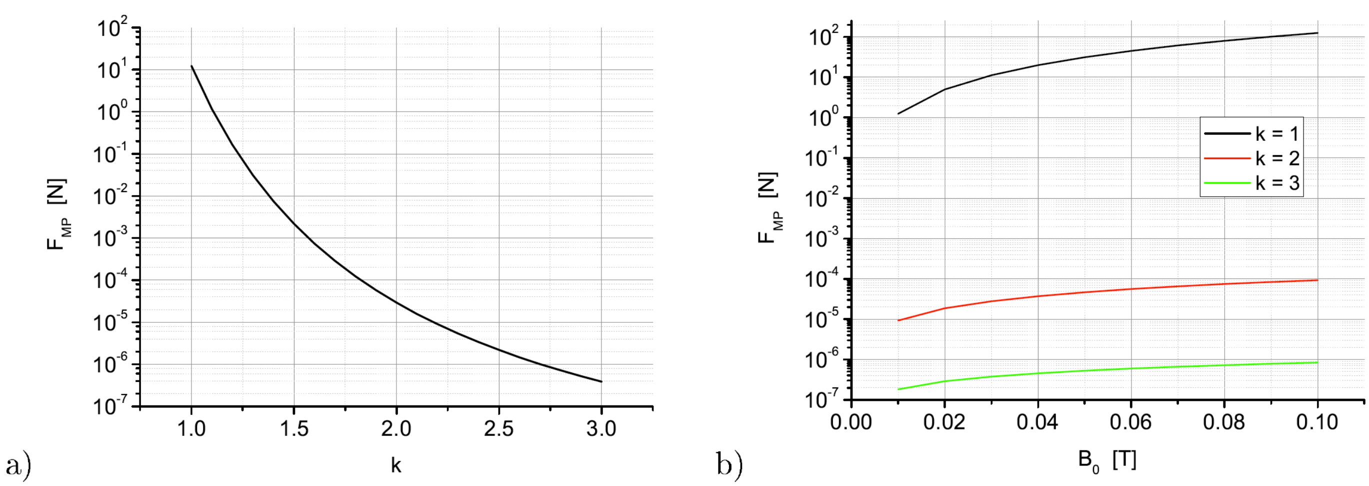

Fig. (4). $F_{MP_{M2P2}}$ based on the values of Winglee and the following relations (see section 3.3): **a)** $F_{MP_{M2P2}}(k)$ and **b)** $F_{MP_{M2P2}}(B_0)$ for different *k*.

$$R_{MP_{M2P2}} = \left(\frac{m}{\pi}\right)^{1/3} B_0^{1/k-1/3} \mu_0^{1/3-1/2k} p_{SW}^{-1/2k} 2^{-1/2k-2/3}, \quad (20)$$

and for the force on the magnetosphere,

$$\begin{aligned} F_{MP_{M2P2}} &= p_{SW} \pi R^2_{MP_{M2P2}} \\ &= \left(\pi m^2\right)^{1/3} 2^{-1/k-4/3} p_{SW}^{1-1/k} \mu_0^{2/3-1/k} B_0^{2/k-2/3}. \end{aligned} \quad (21)$$

Using the values applied by Winglee *et al.* ($I_{coil} = 10\,\mathrm{A}$, $n_{coil} = 1000$, and $d_{coil} = 0.1\,\mathrm{m}$), one gets $m = nIA = 310\,\mathrm{mA}^2$ and $B_0 = 0.03\,\mathrm{T}$. At this point, a first discrepancy is observed. Using the decay parameter applied by Winglee ($k = 1 \Rightarrow F_{MP} \approx 12\,\mathrm{N}$) a similar force is obtained $F_{MP} \approx 5\,\mathrm{N}$. However, using Khazanov's decay parameter ($k = 2$) leads to $F_{MP} \approx 2 \cdot 10^{-5}\,\mathrm{N}$ which is a difference of 6 orders of magnitude (!). The Figs. (**3**, **4**) show the dependence of the magnetopause distance R_{MP} and the force F_{MP} on the decrease parameter k. Fig. (**a**) indicate that for small changes of k the change in F_{MP} and R_{MP} could be some magnitudes. So a precise value of k for investigations of the M2P2 system is essential. Fig. (**b**) shows that the effects of the magnetic field B_0 on the magnetopause and the force are less important than the effects of the k.

Another problem is associated to the force estimation on basis of the currents in the magnetosphere. Then

$$\begin{aligned} F_{SC_x} &\sim \frac{mB_{MP}}{R_{MP}} \sim \mu_0^{1/6+1/2k} B_0^{1/3-1/k} m^{2/3} p_{SW}^{1/2+1/2k} \\ &= f\left(\mu_0, B_0, m, p_{SW}\right) \end{aligned}$$

should be equal to the result of the other derivation, but $F_{MP} \neq F_{SC}$. This is because the induced currents (here mainly the Chapman-Ferraro current) are at a large distance (R_{MP}) from the spacecraft. Thus, the force on the magnetosphere is not equal to the force on the spacecraft. The real force on the spacecraft is therefore smaller than the force on the magnetosphere.

These problems are illustrated in Fig. (**5**). For $k = 1$, the difference between the two derivations is of the order of 10^{11}. For $k = 3$ the results are identical. This is a strong discrepancy between the two derivations in contrast to the simple magnetic sail configuration, i.e. without plasma injection.

The deviation arises because B_{MP} is not changed but R_{MP} is increased [15]. Consequently, the force on the spacecraft decreases even if the size of the magnetosphere increases. This can be explained by the fact that the magnetic field generated by the currents at R_{MP} is smaller in the vicinity of the coil if R_{MP} is large. This results from the simplification $\partial_x B_z(0) \sim B_{MP} / R_{MP}$. Furthermore, the assumption that only the Chapman-Ferraro current is relevant in the magnetosphere is a simplification. There is a whole set of currents existing also next to the spacecraft [14, 15]. Therefore, there are additional forces which cannot be estimated analytically. Finally, the force on the magnetosphere does not equal the force on the spacecraft which motivates further studies with respect to the complex current system.

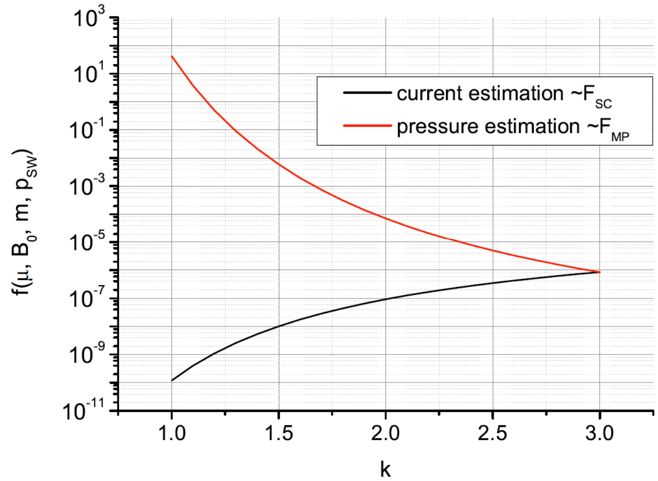

Fig. (5). The relation of F_{SC} (*current estimation*) and F_{MP} (*pressure estimation*) with the function $f\left(\mu_0, B_0, m, p_{SW}\right)$.

4. REQUIREMENTS FOR AN ACCURATE THEORETICAL APPROACH FOR M2P2

On the basis of the previously illustrated it is clear that, analytically, a reliable force information cannot be derived due to the complexity of the current system. Several researchers have tried to tackle the M2P2 problem numerically making use of a MHD approach [9] and a hybrid (MHD/kinetic) approach [4]. The presented analysis shows that comparison of results is prohibited due to a very strong dependence of the forces as well as of the magnetopause on the field decay parameter k which is very differerent in [9] compared with the one in [4]. Although it was shown in section 3.1 that a continuum approach (MHD) is unfeasible to treat the M2P2 problem in general, one cannot conclude that the results obtained in [4] are reliable as it was shown that the hybrid approach suffers of several shortcomings as well. Hence, we discuss possible improvements of the hybrid approach as well as the application of a fully kinetic approach in order to obtain reliable data on M2P2.

4.1. Improved Hybrid Approach

Concerning the first issue (subsection 3.2., static boundary) a hybrid approach should be able to adapt the domain boundary automatically and during run time. This demands grids which are administrated in an unstructured way. Secondly, even if both domains are simulated simultaneously instead of subsequently, this would not solve the issue with the one-way coupling. Clearly, a two-way communication of the electrons would lead to an improvement. However, neither the electron information nor the magnetic field information should be considered as a sufficient condition for a successful M2P2 simulation - the ion energy distribution needs to be fed back into the MHD domain. Since the hybrid approach couples an Eulerian (inner domain, MHD) with a partially Lagrangian approach (outer domain, ions kinetic and electrons fluidic) the ion information has to be sampled in order to avoid numerical instabilities caused by statistical scattering inherent to kinetic methodologies. The sampling could be realized making use of the so-called Information Preservation method, see e.g. [21]. This method demands additional modelling in order to communicate the ion's state to the MHD domain.

Alternatively, one could apply a fully kinetic approach in order to avoid the algorithmic problems related to the coupling of an Eulerian and an Langrangian method.

4.2. Fully Kinetic Approach

The fundamental equation is the gaskinetic Boltzmann equation which describes the statistical distribution of particles in a fluid:

$$\left(\frac{\partial}{\partial t}+\vec{v}\frac{\partial}{\partial \vec{x}}+\frac{\vec{F}}{m}\frac{\partial}{\partial \vec{v}}\right)f(\vec{x},\vec{v},t)=\left.\frac{\partial f(\vec{x},\vec{v},t)}{\partial t}\right|_{coll}. \tag{22}$$

Here, $f(\vec{x},\vec{v},t)$ is the single particle distribution function at location $\vec{x}$, at time t, with velocity $\vec{v}$. Furthermore, $\vec{F}$ is an external force and m is the mass of the particles. The term on the right-hand side is called the collision term to describe the collision effects between particles. This term is the reason for the huge mathematical difficulties in solving the Boltzman equation [22]. Analytical solutions exist only for very special cases such that in general cases a solution can be obtained only numerically. Corresponding kinetic approaches have been developed on basis of a consideration of different spatial scales which are related to certain plasma phenomena.

4.2.1. Non-Collisional Long-Range Interactions

As mentioned, the RHS of the Boltzmann equation represents the influence of collisional effects on the evolution of the particles velocity distribution function. In most plasmas collisional effects are relevant only on very small spatial scales commonly associated with the Debye length [20, 22] which describes the plasma state. On scales above the Debye length plasma behaviour is dominated by collective plasma phenomena which allows to neglect direct Coulomb collisions. Consequently, the right part of Eq. (22) is set to zero which reduces the Boltzmann equation to the Vlasov equation:

$$\left(\frac{\partial}{\partial t}+\vec{v}\frac{\partial}{\partial \vec{x}}+\frac{e}{m}\left(\vec{E}+\frac{1}{c}\left[\vec{v}\times\vec{B}\right]\right)\frac{\partial}{\partial \vec{v}}\right)f(\vec{x},\vec{v},t)=0. \tag{23}$$

Here e is the electron charge, c is the speed of light and $\vec{E}(\vec{x},t)$ respectively $\vec{B}(\vec{x},t)$ are the collective electric field and the collective magnetic field at location $\vec{x}$ at time t of all plasma particles. Self consistency is obtained when the spatial and energetic distribution of charges leads to electric and magnetic forces (represented by $\vec{F}$) which again act on the charges, leading to another distribution and so on. A widely used approach for solving the Vlasov equation is Particle-In-Cell (PIC), see e.g. [23]. In case of M2P2, the description of the magnetic fields is of special interest. The equilibrium between solar wind and magnetosphere could eventually be treated by a magnetostatic approach. Nevertheless, the solution of the full set of Maxwell's equations is most probably essential due to the following issues:

- A time-accurate solution of the Maxwell equations allows for a detailed study of the attachment and detachment process of charges with respect to the magnetic field lines of the magnetic bubble. This concerns issues like the necessary amount of fuel or the parameters for the plasma generator.
- The induced currents influence each other which affects the time dependence of ε_3. This parameter needs to be known for mission scenario analysis.
- The question of the optimal plasma injection direction $(\vec{v}\angle\vec{B})$ to generate the largest possible magneto-sphere requires an exact study of the evolution of the magnetosphere. This is also necessary for temporal changes of $\vec{B}$. Only the solution of the complete set of the Maxwell equations might clarify whether there is such an effect or not.

4.2.2. Collisional Long-Range Interactions

Coulomb collisions are typically neglected in common plasmas as the respective spatial scales at which these effects are relevant are far too small. However, due to the small plasma density in space the corresponding scaling is different such that a consideration of electron relaxation effects may become reasonable. Otherwise the assumption of a non-collisional plasma inherent to the Vlasov theory is not fulfilled. A typical measure for the spatial resolution is given by the Debye length. On scales much larger than the Debye length only collective plasma phenomena are considered and the Vlasov equation is valid. Such a situation is expected to occur in the outer region of the M2P2 system where the plasma density is very low. In the region of the plasma injection this is presumably not the case. Moreover, as it is unknown *a priori* how the system evolves in time one can expect to have cells over-resolved, and other cells under-resolved. Avoiding a dynamical grid adaptation one needs to decide individually for each cell how to proceed, i.e. which plasma phenomena need to be taken into account. In such a case one would have to solve the Fokker-Planck equation (FP)

$$\begin{aligned}\left.\frac{\partial f(\vec{x},\vec{v},t)}{\partial t}\right|_{coll} &= -\sum_{i=1}^{3}\frac{\partial}{\partial v_i}\left[A_i f(\vec{x},\vec{v},t)\right]\\ &\quad+\frac{1}{2}\sum_{i,j=1}^{3}\frac{\partial^2}{\partial v_i \partial v_j}\left[B_{i,j} f(\vec{x},\vec{v},t)\right]\end{aligned} \tag{24}$$

which can be deduced from the Boltzmann equation in the limit of small angle Coulomb scattering processes. Here $A_i = A_i(\vec{x},\vec{v},t)$ is the dynamic friction coefficient and $B_{i,j} = B_{i,j}(\vec{x},\vec{v},t)$ is the dynamic diffusion coefficient. A highly efficient method for solving this equation was developed by Nanbu [24]. Once the electron relaxation needs to be resolved, an algorithmic proceeding could look like this:

1. The Coulomb collisions should be considered if the Debye length is resolved. In this case, it cannot be assumed that there are no direct Coulomb collisions (Vlasov theory).
2. If the Debye length is not resolved, the Vlasov theory is valid and formally the collective plasma phenomena are dominating. However, the Vlasov theory does not describe chemical processes which are based on short range interactions.
   (a) The direct Coulomb collisions do not need to be resolved if an equilibrium distribution of energy of electrons is present.
   (b) The electron relaxation processes (*via* direct Coulomb collisions) need to be resolved in case that the equilibrium distribution of the electrons is strongly disturbed. This allows for a physically more exact study of e.g. the production of new charges which again populate the distribution function $f(\vec{x},\vec{v},t)$ described by the Vlasov equation.

In case of 2.b) it is proposed to use the dimensionless Damköhler number Da which might be applicable as an indicator for a resolution of the electron relaxation (see Table **2**). Da is the ratio of retention time of a species in a volume (here, cell size/flow rate of electrons) and relaxation time of the interaction (here, reciprocal of $(e;e)$ collision frequency). Initially, sensitivity studies should be made to study the influence of the electron energy distribution on the rate coefficients for charge producing processes. The computation of electron relaxation in an under-resolved cell is not necessary if the disturbance of the equilibrium distribution of electron energy has a negligible influence on the chemical processes. Otherwise, a criterion must be found which characterises the quality of the disturbance according to the influence on the respective plasma chemical processes.

Table 2. Reaction Zones and Related Damköhler Numbers [25, 26]

Chemical Reaction Zone	Progress of the Reaction	Damköhler Number Da
equilibrium	reaction follows distortion-free t he state of flow	$Da > 100$
non-equilibrium	reaction follows delayed the state of flow	$0.01 < Da < 100$
frozen	no reaction/reaction path to long	$Da < 0.01$

4.2.3. Collisional Short-Range Interactions

The RHS of Eq. (22) represents only binary collisions. Taking into account that gravity has a negligible effect on particle movement and that neutrals are not affected by electric and magnetic fields, the force term on the LHS vanishes and one gets the simplified Boltzmann equation. This equation has to be solved for the short-range interactions, e.g. in case of neutral-neutral or electron-neutral interactions. For technical, i.e. large scale problems, a feasible methodology could be the Direct Simulation Monte Carlo method (DSMC). A detailed description can be found e.g. in [22]. As mentioned, a plasma jet is injected at the dipole in order to expand the magnetic bubble. This area is of high density compared with the other M2P2 regions. In fact, chemistry processes are expected to be of importance in this region.

4.3. Performance Aspects

Of course, there are performance issues with a fully kinetic simulation which need to be addressed adequately. Precisely, the required performance to simulate a huge number of particles is limiting the feasibility of complex problems. Assuming that PIC, DSMC, and FP are required - each of these solvers has a linear dependency $\mathcal{O}(n)$ with respect to the number of particles in the simulation (FP solver based on Monte Carlo Simulation). According to the densities used by Khazanov *et al.* [4], we estimate that for a simulation of M2P2 in a cube of $80 \times 80 \times 80\ \mathrm{km}^3$ about 10^{23} real particles are necessary. With the typical amount of memory available on super computers it should be possible to treat about 10^9 particles. This would lead to macro particle factors of about 10^{14}, i.e. each simulated particle represents 10^{14} real particles. It is well-known that high macro particle factors induce other problems as the macro particle factor is nothing else than an additional discretization step. In PIC, charges would need to be smeared in order to prevent corresponding instabilities, see e.g. [27]. In DSMC, a high particle factor affects interaction probabilities in correlation with the spatial and temporal resolution, as well as the averaging of macroscopic quantities. So far it is not known how the particle discretization affects the FP solution.

Given the abovely discussed solver specific domains of considered phenomena, each of the three solvers works on different spatial scales: PIC above the Debye length, FP below the Debye length, and DSMC below the mean free path. So, the mean free path and/or the Debye length should be resolved in the inner region of the M2P2 domain. On the other hand, such a high refinement in the outer region where only the Vlasov equation needs to be solved would lead to unreasonable computational complexity. On the basis of the traditional way of discretizing space, at least two different and adaptive meshes have to be maintained which is time and memory consuming. Here, improved methodologies would be favourable.

Another problem of the fully kinetic simulation is the very large temporal scale difference for the different solvers. In case of an explicit time-accurate PIC solver, the speed of light needs to be resolved leading to time step sizes in the order of $10^{-12}\,\mathrm{s}$ and even smaller, depending on the cell size. This is correlated with the corresponding CFL (Courant-Friedrichs-Lewy) condition. The minimum time step size necessary in DSMC is caused by the short range collisional process in a plasma to resolve and is typically in the order of $10^{-7} - 10^{-10}\,\mathrm{s}$. Moreover, the Monte Carlo based FP solver has no strict time constraint. The choice of time step size depends on the electron relaxation phenomena which the user would like to resolve in detail. Given that, the time step sizes to be applied are very heterogeneous.

The integration of equations of motion is also affected by the time scale differences. Electron movement is coupled with the field computation in a very complex way, even more in case of relativistic effects, see e.g. [28]. Similar holds for ions which are usually much slower though. Both charged species types demand a high-order integration in order to provide energy conservation on large scales. Hence, the integration algorithm needs to be symplectic. This would also allow for a larger time step size for the integration step.

Advanced numerical techniques like variable and local time stepping, sub-cycling, efficient vectorization and parallelization would relieve these performance issues related to a fully kinetic multi-scale approach. However, the main performance improvement can be expected by making the PIC solver implicit, since if explicit the speed of light in a time-accurate PIC solver would define the minimum global time step.

5. CONCLUSIONS

The motivation for this article has been to evaluate previous studies on magnetic sail concepts. In this context, two analytical approaches without plasma injection are discussed and explained. These two approaches are applied on the M2P2 concept and the results are compared with the studies of Winglee *et al.* [3] and Khazanov *et al.* [4]. It is shown that significant discrepancies are present between the results of a MHD approach (Winglee), a hybrid approach (Khazanov), and the expected results of the analytical estimations. Therefore, the validity of the MHD approach is critically discussed, with the result that the MHD approach cannot be used at all scales of the simulation. However, also the disadvantages of the hybrid approach are shown, e.g. the static border or the incomplete information exchange between the domains. Due to these results, a fully kinetic simulation is proposed as a more accurate numerical approach for M2P2. Here, the requirements of such a simulation are clarified and the necessary numerical solvers are briefly discussed.

REFERENCES

[1] Barrie A. M2P2 using variable power radial thrust for interplanetary and interstellar travel. Technical report, American Institute of Aeronautics and Astronautics 2006.

[2] Cummings H, Ross M, Welsh D, *et al*. Incorporation of the Mini magnetospheric plasma propulsion system (M2P2) in a manned mission to mars. Technical report, Department of Aeronautics and Astronautics University of Washington and Department of Geophysics University of Washington 2001.

[3] Winglee RM. Mini magnetospheric plasma propulsion (M2P2) final report. Technical report, University of Washington, 1999.

[4] Khazanov G, Delamere P, Kabin K, Linde TJ. Fundamentals of the plasma sail concept: magnetohydrodynamic and kinetic studies. J Propuls Power 2005; 21:853-61.

[5] Funaki I, Yamakawa H. Research status of sail propulsion using the solar wind. J Plasma Fusion Res 2009; 8:1580-4.

[6] Winglee RM, Slough J, Ziemba T, *et al*. Large scale mini magnetospheric plasma propulsion (M2P2) experiments. Technical report, ESA 2001.

[7] Ueno K, Kimura T, Ayabe T, Funaki I, Horisawa H, Yamakawa H. Laboratory experiment of magneto plasma sail, part 1: pure magnetic sail. In: The 30th International Electric Propulsion Conference 2007.

[8] Kimura T, Ueno K, Ayabe T, *et al*. Laboratory experiment of magneto plasma sail, part 2: magnetic field infation. In: The 30th International Electric Propulsion Conference 2007.

[9] Winglee RM, Slough J, Ziemba T, Goodson A. Mini magnetospheric plasma propulsion: tapping the energy of the solar wind for spacecraft propulsion. J Geophys Res 2000; 105:21067-77.

[10] Nishida H, Funaki I, Ogawa H, Inatani Y. MHD analysis on propulsive characteristics of magneto plasma sail. In: The 30th International Electric Propulsion Conference 2007.

[11] Zubrin R. The magnetic sail. Technical report, NASA Institute of Advanced Concepts 2000.

[12] Kivelson MG, Russell CT. Introduction to space physics. Cambridge: Cambridge University Press 1995.

[13] Ivory K. Suprathermische Elektronen im Sonnenwind als Indikatoren aussergewoehnlicher Magnetfeldstrukturen der inneren Heliosphaere. PhD thesis, Georg-August-Universitaet Goettingen 1998.

[14] Kallenrode MB. Space physics. Berlin: Springer 2004.

[15] Toivanen PK, Janhunen P, Koskinen HEJ. Magnetospheric propulsion (eMPii). Technical report, ESA ESTEC 2004.

[16] Baumjohann W, Treumann RA. Basic space plasma physics. London: Imperial College Press 1997.

[17] Alfven H, Fuelthammar CG. Cosmical electrodynamics: fundamental principles. Oxford, England: Oxford Press 1963.

[18] Herdrich G. Habilitation: Raumfahrtrelevante Plasmen und deren anwendungsbezogene Klassizierung. Fakultaet Luft- und Raumfahrttechnik und Geodaesie der Universitaet Stuttgart 2011.

[19] Cattell C, Catto P, Funsten H, *et al*. Physics and technology of the feasibility of plasma sails. J Geophys Res 2005.

[20] Cap F. Lehrbuch der Plasmaphysik und Magnetohydrodynamik. Berlin: Springer 1994.

[21] Carlson HA, Roveda R, Boyd ID, Candler GV. A hybrid CFD-DSMC method of modeling continuumrarefed flows. In: 42nd AIAA Aerospace Sciences Meeting and Exhibit Reno 2004.

[22] Bird GA. Molecular gas dynamics. Oxford: Clarendon Press 1976.

[23] Birdsall CK, Langdon AB. Plasma physics *via* computer simulation. Taylor and Francis, 2004.

[24] Nanbu K. Probability theory of electronmolecule, ionmolecule, moleculemolecule, and coulomb collisions for particle modeling of materials processing plasmas and gases. IEEE Trans Plasma Sci 2000; 28:971-990.

[25] Koppenwallner G. Aerodynamik des Wiedereintritts. Hyperschall Technologie Goettingen 2005.

[26] Kanne S. Zur thermo-chemischen Relaxation innerer Freiheitsgrade durch Stoss- und Strahlungsprozesse beim Wiedereintritt. VDI, Verlag 2000.

[27] Jacobs GB, Hesthaven JS. Highorder nodal discontinuous galerkin particleincell method on unstructured grids. J Comput Phys 214:96-121, 2006.

[28] Quandt M. Dissertation: high order particle transport for pic simulations of plasma flows. PhD thesis Universitaet Stuttgart 2010.

Received: February 16, 2011 Revised: April 20, 2011 Accepted: April 20, 2011